The Astrophysical Journal Letters, 907:L2 (5pp), 2021 January 20 https://doi.org/10.3847/2041-8213/abd567

Turbulence and Particle Acceleration in Shearing Flows

Frank M. Rieger[1,2] and Peter Duffy[3]
[1] ZAH, Institute of Theoretical Astrophysics, University of Heidelberg Philosophenweg 12, D-69120 Heidelberg, Germany; f.rieger@uni-heidelberg.de
[2] Max-Planck-Institut für Kernphysik, Saupfercheckweg 1, D-69117 Heidelberg, Germany
[3] School of Physics, University College Dublin, Belfield, Dublin 4, Ireland
Received 2020 October 29; revised 2020 December 1; accepted 2020 December 21; published 2021 January 14

Abstract

We explore constraints imposed by shear-driven instabilities on the acceleration of energetic particles in relativistic shearing flows. We show that shearing layers in large-scale AGN jets are likely to encompass a sizeable fraction ($\gtrsim$0.1) of the jet radius, requiring seed injection of GeV electrons for efficient acceleration. While the diffusion process may depend on predeveloped turbulence if injection occurs at higher energies, electron acceleration to PeV and proton acceleration to EeV energies appears possible within the constraints imposed by jet stability.

Unified Astronomy Thesaurus concepts: High energy astrophysics (739); Non-thermal radiation sources (1119); Active galactic nuclei (16); Radio jets (1347); Relativistic jets (1390)

1. Introduction

The jets from active galactic nuclei (AGN) exist from subparsec to megaparsec scales (see Blandford et al. 2019 for a recent review). While apparently relativistic and unidirectional, the underlying flow is likely to exhibit some transverse velocity stratification already close to its origin (e.g., Rieger & Duffy 2004). As these jets then continue to propagate, interactions with the ambient medium can excite instabilities and induce mixing and mass loading, thereby enforcing further velocity shearing (see Perucho 2019 and references therein). Differences in jet speeds V_j and Mach numbers M_j in this regard are expected to contribute to the observed morphological differences of Fanaroff–Riley (FR) I and II sources, respectively (see Martí 2019). The growing realization of velocity shearing has in recent times motivated a variety of studies exploring its consequences for nonthermal particle acceleration and emission (e.g., Tavecchio & Ghisellini 2015; Rieger & Duffy 2016, 2019; Liang et al. 2017; Chhotray et al. 2017; Liu et al. 2017; Kimura et al. 2018; Webb et al. 2018, 2019, 2020; Tavecchio 2021). Radio observations of AGN indeed provide evidence for a spine-sheath-type jet structure on subparsec as well as on kiloparsec scales (e.g., Perlman et al. 1999; Laing & Bridle 2014; Mertens et al. 2016; Giovannini et al. 2018).

On large scales, the survival of AGN jets is presumably largely determined by their response to the Kelvin–Helmholtz instability (KHI; e.g., Turland & Scheuer 1976; Blandford & Pringle 1976; Birkinshaw 1996; Ferrari 1998; Trussoni 2008; Hardee 2013). Macroscopic KHIs can develop between two fluids in relative motion as present, for example, at the interface of a jet with its ambient medium. The physical cause is related to the Bernoulli equation: if a ripple forms at the interface, the fluid has to flow faster to pass over it and thus exerts less pressure, allowing the ripple to grow further. This can result in mixing of the fluids and an effective transfer of momentum across the interface, leading to shearing, decollimation, and deceleration of the jet. The excitation of long-wavelength KHI modes can affect the jet morphology, while short-wavelength modes can lead to a turbulent cascade conducive to in situ particle acceleration (e.g., Ferrari et al. 1979). In the present Letter we are interested in whether stochastic shear particle acceleration can occur under conditions for which the jet stability itself is not affected.

Fast shear flows can facilitate energetic particle acceleration by several means (see Rieger 2019 for a recent review). One of the best studied possibilities includes a stochastic Fermi-type process, in which particle energization occurs as a result of elastically scattering off differentially moving (magnetic) inhomogeneities embedded in a shearing background flow (e.g., Berezhko & Krymskii 1981; Earl et al. 1988; Webb 1989; Rieger & Duffy 2006; Lemoine 2019). The scattering center's speeds are then essentially defined by the general shear flow profile, and the efficiency determined by the flow difference sampled over one particle mean free path. While a strong (fast and narrow) shear layer may thus appear more favorable for particle acceleration, it could also be at the same time more KHI unstable.

Given recent developments, this Letter explores the regime for which both jet stability and efficient shear particle acceleration are ensured. Its prime focus is on large-scale AGN jets whose macroscopic stability properties are accessible to a hydrodynamical description. This allows for a complementary view compared to a microscopic PIC approach (e.g., Sironi et al. 2020).

2. Shear Instabilities and Turbulence

Extragalactic radio jets are generally characterized by high Reynolds numbers, possibly reaching Re $\sim 10^{28}$ (Birkinshaw 1996). Hence, even if initially laminar, the flows are expected to quickly develop turbulent boundary layers that spread inward and facilitate entrainment of ambient matter (e.g., De Young 1993). As a result of mixing, the shear layer widens, suggesting that its lateral extent increases with distance along the jet. While the physical nature of the transverse momentum transport (giving rise to internal friction/viscosity) in relativistic jets is not yet understood, it presumably involves turbulent eddy as well as cosmic-ray viscosity (i.e., associated with energetic particle acceleration; e.g., Earl et al. 1988; Rieger & Duffy 2006; Webb et al. 2019). The boundary layer, on the other hand, is likely to be shaped by the nonlinear growth of unstable Kelvin–Helmholtz (KH) modes. The excitation of unstable, macroscopic KH modes in relativistic, kinetically dominated cylindrical jets has been studied, both by

analytical and numerical means, in the vortex-sheet approximation as well as for sheared flows (e.g., Hardee 1979; Birkinshaw 1991; Hanasz & Sol 1996; Hardee et al. 1998; Urpin 2002; Perucho et al. 2004, 2005; Perucho & Martí 2007; Rossi et al. 2008). The initially exponentially growing modes inferred from linear stability analysis could disrupt or deform the jet if nonlinear saturation does not occur. Numerical simulations in fact indicate that jets with high Lorentz factors and large Mach numbers could get stabilized by the presence of a shear layer due to various nonlinear effects (e.g., shear-layer resonances; e.g., Perucho et al. 2007).

The present Letter provides a first attempt to relate macroscopic, shear-driven, KH-type instabilities to shear particle acceleration, and explores its consequences for the layer width and the particle acceleration efficiency. Following Urpin (2002), we can get insights into the related KHI growth times by means of some basic physical considerations. For convenience, we assume a cylindrical relativistic jet with outer radius R_j and smoothly varying (yet still relativistic) velocity shear profile $V_j(r)\vec{e}_z$. Due to the longitudinal bulk shear, the emergence of a small velocity perturbation $v_{1,r}$ in the radial direction will induce a perturbation in the z-direction, $dv_{1,z}/dt \simeq -v_{1,r}\,(dV_j/dr)$. Denoting the characteristic timescale of this process by τ, we can write

$$v_{1,z} \simeq -\tau\, v_{1,r}\,(dV_j/dr). \tag{1}$$

Following the (linearized) continuity equation, velocity perturbations are related to density perturbations by $\frac{\partial \rho_1}{\partial t} \simeq -\rho\,(\partial/\partial z)v_{1,z}$, or $\frac{\rho_1}{\tau} \simeq -\rho\, v_{1,z}\, k$, where k is the longitudinal wavenumber, so that

$$\rho_1 \simeq \rho\, k\tau^2 v_{1,r}(dV_j/dr). \tag{2}$$

Since density perturbations are accompanied by pressure perturbations, $p_1 = c_{sj}^2\,\rho_1$ (adiabatic case), we have

$$p_1 \simeq c_{sj}^2\,\rho\, k\tau^2 v_{1,r}\,(dV_j/dr). \tag{3}$$

Pressure forces, on the other hand, can change the radial velocity, $\Gamma_j^2\rho\,(v_{1,r}/\tau) \simeq -(\partial p_1/\partial r)$, according to the (linearized) relativistic momentum equation, so that

$$\frac{v_{1,r}}{\tau} \simeq -\frac{1}{\rho\Gamma_j^2}\frac{\partial}{\partial r}[c_{sj}^2\,\rho\, k\tau^2 v_{1,r}\,(dV_j/dr)], \tag{4}$$

where $\Gamma_j(r) = 1/(1 - V_j(r)^2/c^2)^{1/2}$ is the bulk flow Lorentz factor. Following Urpin (2002) the radial change in the growth rate scales with velocity gradient as $\frac{\partial}{\partial r}(1/\tau) \sim k(dV_j/dr)$, so that $(\partial\tau/\partial r) \sim -k\tau^2(dV_j/dr)$. Hence, one finds that the (instability) growth rate in the galaxy rest frame becomes

$$\frac{1}{\tau} \simeq \sqrt{\frac{\sqrt{2}\,c_{sj}k(dV_j/dr)}{\Gamma_j}} \simeq \sqrt{\frac{\sqrt{2}\,c_{sj}c\;k(d\Gamma_j/dr)}{\Gamma_j^4}}, \tag{5}$$

where $dV_j/dr = (c^2/V_j)\quad (d\Gamma_j/dr)(1/\Gamma_j^3) \simeq c(d\Gamma_j/dr) \times (1/\Gamma_j^3)$ has been used on the right-hand side. This expression agrees with the more detailed derivation (Equations (26) and (41) in Urpin (2002). It implies a length scale L at which a relativistic shear flow may get significantly destabilized of

$$L \simeq c\tau^* \simeq \Gamma_j^{3/2}\sqrt{\frac{c}{c_{sj}}\Delta R_j\frac{\Gamma_j}{(d\Gamma_j/dr)}} \sim \Gamma^{3/2}\Delta R_j\sqrt{\frac{c}{c_{sj}}}, \tag{6}$$

assuming $\tau^* = 3\tau$, $k \simeq 2\pi/\Delta R_j$, a shear width $\Delta R_j \leqslant R_j$, and $d\Gamma_j/dr \sim \Gamma_j/\Delta R_j$. For $\Gamma_j = 10$, $\Delta R_j \sim R_j = 100$ pc and $c_{sj} = c/10$, for example, this would yield $L \sim 10$ kpc. Equation (5) implies that the growth time τ increases with Γ_j and $M_j = V_j/c_{sj}$, so that the shear KHI could be suppressed in supersonic, highly relativistic jets. On the other hand, the instability arises faster for perturbations with shorter axial wavelengths, $\tau \propto 1/k^{1/2}$, suggesting that jets could possibly be made turbulent by shear stresses. Requiring a jet length-to-width ratio $L/R_j \geqslant 10$, Equation (6) can be used to estimate the required shear width,

$$\left(\frac{\Delta R_j}{R_j}\right) \gtrsim 0.1\left(\frac{10}{\Gamma_j}\right)^{3/2}\left(\frac{10}{M_j}\right)^{1/2}. \tag{7}$$

We note that this is compatible with recent findings for the large-scale jet in S5 0836+719 (Vega-García et al. 2019). Equation (7) suggests that in the absence of other stabilizing effects, narrow ($<0.1R_j$) shear layers are unlikely to exist around the kiloparsec-scale jets of AGN, and this could be of relevance for understanding the potential of shear particle acceleration.

3. Shear Particle Acceleration

Fast shear flows can facilitate a stochastic Fermi-type acceleration of energetic ($v \simeq c$) charged particles as these particles diffuse across the flow and sample the differences in flow speed (see Rieger 2019 for a recent review). Gradual shear acceleration generally requires relativistic flow speeds ($\Gamma_j >$ a few) to be efficient (Webb et al. 2018; Rieger & Duffy 2019), and this makes an application to AGN jets particularly interesting.

For the relativistic shear flow profile considered above, $V_j(r)\vec{e}_z$, the characteristic (comoving) shear acceleration timescale can be expressed as (e.g., Rieger 2019)

$$t'_{\rm acc}(p') = \frac{c}{(4+\alpha)\tilde{\Gamma}_s\,\lambda'} \propto p'^{-\alpha}, \tag{8}$$

where $\lambda'(p') = c\,\tau'_s(p')$ is the energetic particle mean free path, $\tau'_s(p')$ is the (momentum-dependent) mean scattering time, assumed to follow a parameterization $\tau'_s(p') = \tau'_0(p'/p'_0)^\alpha$, with $p' = \gamma' mc$ the comoving particle momentum, and $\tilde{\Gamma}_s$ is the shear coefficient given by (Rieger & Duffy 2004; Webb et al. 2018)

$$\tilde{\Gamma}_s = \frac{1}{15}\,\Gamma_j(r)^4\left(\frac{\partial V_j}{\partial r}\right)^2. \tag{9}$$

In general, the acceleration timescale depends on both the particle momentum and the radial coordinate. Equation (9) indicates that a strong velocity shear (i.e., large gradients) will be favorable for particle acceleration. Equation (7), on the other hand, constrains ΔR_j to be above some threshold for a given source. Since λ appears in the denominator of Equation (8), shear acceleration of electrons generally requires seed injection of some preaccelerated electrons to be efficient, i.e., to proceed within the lifetime of the system. One can estimate the required seed energies ($\gamma'_{\rm min}$) by equating the acceleration timescale $t_{\rm acc}(r_0)'$ (or a multiple η of it) with the (comoving) dynamical

timescale, i.e., $\eta t'_{\rm acc} = t'_{\rm dyn} \equiv L/\Gamma_j V_j$, with $\eta > 1$. As before (e.g., Liu et al. 2017; Rieger & Duffy 2019), we use a quasi-linear-type parameterization for the particle mean free path in the shear, i.e.,

$$\lambda' \simeq \xi^{-1} r'_g \left(\frac{r'_g}{\Lambda_{\rm max}}\right)^{1-q} \propto \gamma'^{2-q}, \quad (10)$$

where $\xi \leqslant 1$ denotes the energy density ratio of turbulent versus regular magnetic field B', $\Lambda_{\rm max}$ is the longest interacting wavelength of the turbulence, $r'_g = \gamma' mc^2/eB'$ is the particle Larmor radius, γ' the comoving particle Lorentz factor, and q is the power index of the turbulence spectrum (e.g., $q = 5/3$ for Kolmogorov-type turbulence). For the chosen notation, $\alpha = 2 - q$, i.e., $\alpha = 1/3$ for a Kolmogorov-type turbulence. We note that while Equation (10) provides a first approach, in general appropriate numerical simulations are needed to properly quantify the diffusive particle transport in turbulent shearing flows. Assuming a linearly decreasing velocity profile, $V_j(r) = V_0 - (\Delta V_j/\Delta R_j)(r - r_0)$ with $r_0 = 0$, and $\Lambda_{\rm max} = \Delta R_j$, the above condition results in

$$\gamma'_{\rm min} \geqslant \frac{e\,B' L}{m\,c^2}\left[\frac{15\xi\,\eta}{(4+\alpha)\Gamma_j^3}\left[\frac{c}{\Delta V_j}\right]^2\left(\frac{V_j}{c}\right)\left[\frac{\Delta R_j}{L}\right]^{3-q}\right]^{\frac{1}{2-q}}. \quad (11)$$

Hence, for electrons and $q = 5/3$ one obtains

$$\gamma'_{\rm min,e} \geqslant 3.3 \times 10^3 \left(\frac{B'}{10^{-4}\ {\rm G}}\right)\left(\frac{5}{\Gamma_j}\right)^9 \times \left(\frac{\Delta R_j/L}{50}\right)^4\left(\frac{L}{5\ {\rm kpc}}\right)\left(\frac{\xi\eta}{1.0}\right)^3. \quad (12)$$

For protons, $\gamma'_{\rm min,p} \geqslant \gamma'_{\rm min,e} \times (m_e/m_p)$. Equation (12) indicates that efficient electron acceleration can require substantial seed injection. It seems possible, however, that in many cases the required energetic seed electrons can be provided by classical, first (diffusive shock), and second-order Fermi-type processes (e.g., Liu et al. 2017). Note that given the widths inferred in Equation (7), the operation of nongradual ($\lambda' > \Delta R_j$) shear particle acceleration has a rather high seed energy threshold, and this could affect inferences related to nongradual shear acceleration of pick-up cosmic rays in large-scale AGN jets (e.g., Kimura et al. 2018).

Estimating maximum achievable Lorentz factors $\gamma'_{\rm max,e}$ for electrons by balancing the acceleration timescale with the synchrotron loss timescale, $t'_{\rm acc} = t'_{\rm syn} \equiv (9m^3c^5)/(4e^4\gamma' B'^2)$, suggests that in principle $\gamma'_{\rm max,e} \sim 10^8$ is possible. This makes shear acceleration an interesting candidate for understanding the origin of the extended high-energy emission in the large-scale jets of AGN, such as in, e.g., Centaurus A (H.E.S.S. Collaboration et al. 2020). In the case of protons, on the other hand, synchrotron losses are usually negligible, and achievable energies are instead limited by the condition of lateral confinement, $\lambda' \leqslant \Delta R_j$ (Rieger & Duffy 2019)

In general, efficient shear acceleration requires the presence of sufficient turbulence scattering particles across the flow. As noted before, it seems likely that shear-driven KH instabilities could contribute to the generation of macroscopic turbulence. Numerical simulations of mildly relativistic (counter-propagating), transonic shear flows suggests that KHI vortices could quickly drive electromagnetic turbulence (Zhang et al. 2009). In the following we explore the case where the wavenumber of the KHI unstable modes is related to the energetic particle mean free path. Working in the comoving frame, we employ $k' = 2\pi/\lambda'$ with $k \sim k'/\Gamma_j$. We use relation (5) with $\tau' = \tau/\Gamma_j$ to characterize the relevant (comoving) instability timescale τ', yielding

$$\tau' \simeq (\sqrt{2}\, c_{sj}(2\pi/\lambda')(dV_j/dr))^{-1/2} \propto \gamma'^{\frac{\alpha}{2}}. \quad (13)$$

The (comoving) particle Lorentz factor at which acceleration and turbulence generation would proceed on the same timescale is then given by

$$\gamma'_t = \frac{eB'}{mc^2}\left(\frac{15}{4+\alpha}\right)^2\left(\frac{c}{(dV_j/dr)}\right)^3 \frac{2^{3/2}\pi\xi^3}{\Gamma_j^8 M_j (\Delta R_j)^2}. \quad (14)$$

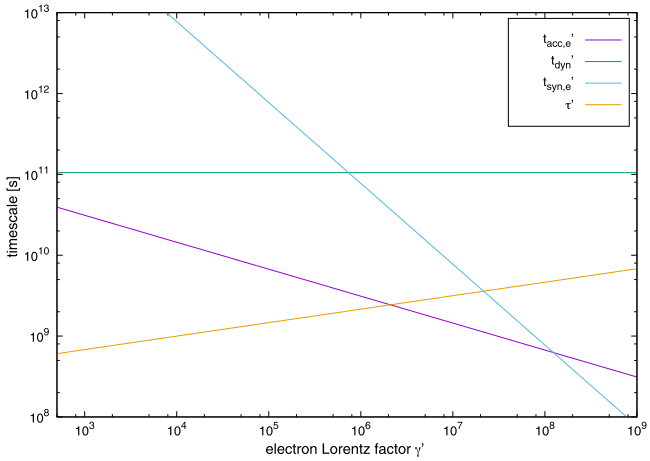

Figure 1. Characteristic (comoving) timescales for electron shear acceleration. The green, blue, purple, and yellow lines denote the dynamical timescale $t'_{\rm dyn}$, the synchrotron loss timescale $t'_{\rm syn,e}$, the electron acceleration timescale $t'_{\rm acc,e}$, and the KHI instability timescale τ', respectively. For the chosen set of parameter $\gamma'_{\rm max,e} \simeq 10^8$ (synchrotron-limited). Parameters used are $L = 5$ kpc, $\Delta R_j = 0.02L$, $B' = 10^{-4}$ G, $\Gamma_j = 5$, $\xi = 0.2$, and $c_{sj} = 0.05$ c.

Figure 1 shows an example of the resultant characteristic timescales as applied to electrons, with $t'_{\rm acc} \equiv t'_{\rm acc}(r_0)$. The maximum electron energy in this case is synchrotron-limited to $\gamma'_{\rm max,e} \simeq 10^8$, and the ratio $t'_{\rm dyn}/\tau(\gamma'_{\rm max,e})' \simeq 22$. For efficient acceleration, seed electron injection with $\gamma'_e \gtrsim 10^3$ would be needed. Over a wide regime $\tau' \ll t'_{\rm dyn}$, suggestive of a fully developed turbulence. For $\gamma'_e \lesssim \gamma'_t \simeq 2 \times 10^6$, local turbulence generation is sustained by proceeding faster than acceleration. For $\gamma'_e \gtrsim 2 \times 10^6$, on the other hand, $\tau' \geqslant t'_{\rm acc,e}$, so that continuous acceleration would depend on predeveloped KHI turbulence. The situation can effectively be stabilized, however, if electron seed injection (γ'_i) occurs sufficiently below γ'_t (e.g., at $\gamma'_i \sim \gamma'_t/5$), as $t_{\rm acc}(\gamma'_i)'$ will set the relevant time threshold. Complementarily, interactions of the jet with stars could possibly provide an additional source of small-scale turbulence for the jet shear layer (e.g., Perucho 2020).

Figure 2 shows an illustration of the resultant characteristic timescales for protons, with $t'_{\rm acc} \equiv t'_{\rm acc}(r_0)$. The dotted line characterizes the regime where, formally, the diffusion approximation employed in gradual shear becomes violated,

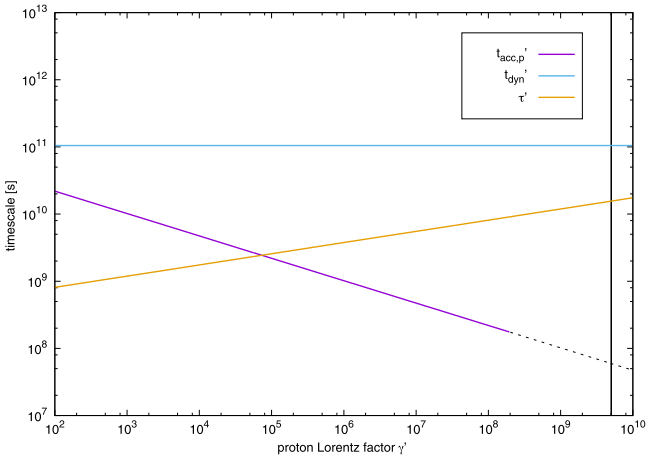

Figure 2. Characteristic (comoving) timescales for proton shear acceleration. The blue, purple, and yellow lines denote the dynamical timescale $t'_{\rm dyn}$, the proton acceleration timescale $t'_{\rm acc,p}$, and the KHI instability timescale τ', respectively. The vertical black line denotes the confinement limit $\gamma'_{\rm max,p} = 5 \times 10^9$. Parameters used are $L = 5$ kpc, $\Delta R_j = 0.02L$, $B' = 10^{-4}$ G, $\Gamma_j = 5$, $\xi = 0.8$, and $c_{sj} = 0.05$ c.

and transition to nongradual shear is expected to occur (cf. Rieger 2019). The maximum proton energy in this case is expected to be limited to $\gamma'_{\rm max,p} = 5 \times 10^9$, and the ratio $t'_{\rm dyn}/\tau(\gamma'_{\rm max,p})' \simeq 7$. Since we anticipate the layer stability (ΔR_j) to be only disrupted after several e-folding times (τ'), such (comoving) energies $\sim\gamma'_{\rm max,p}$ may still be achievable. For seed injection $\gamma'_p \gtrsim \gamma'_t \simeq 7 \times 10^4$, acceleration would depend on predeveloped KHI turbulence or other turbulence driving mechanisms. In principle, significant turbulence damping and jet deceleration might become possible for low jet powers or sufficiently high cosmic-ray seed densities. For example, if a seed density comparable to that of the cosmic rays in our galaxy ($\sim 3 \times 10^{-15}$ cm^{-3}) would be picked up at TeV energies, then this may become apparent for jets with powers $L_j \lesssim 10^{43}$ erg s^{-1}.

4. Conclusion

The foregoing analysis suggests that relativistic AGN jets can get stabilized by the presence of an extended ($\gtrsim 0.1R_j$) shear layer. This inference is based on a simplified linear model of KH-driven shear instabilities in a steady, kinetically dominated flow. In general, KH instabilities may not necessarily destroy the jet configuration, as the system could instead saturate leading to another stable configuration, and inclusion of a parallel magnetic field could contribute to jet stability (e.g., Hamlin & Newman 2013). In addition, the jet stability properties are likely to be affected by the characteristics of the confining medium. While a more complex application is thus desirable and aimed for in further work, we note that our current estimates are compatible with recent experimental findings (Vega-García et al. 2019). As found here, efficient particle acceleration in extended shear layers usually requires seed injection of energetic GeV) electrons. Shear acceleration of electrons (synchrotron-limited) to multi-TeV energies and protons (confinement-limited) to EeV energies seems then feasible in the kiloparsec-scale jets of AGN (Rieger & Duffy 2019). As shown here, shear-driven instabilities could in fact contribute to turbulence generation and thereby facilitate particle acceleration. Relating the particle mean free path to the wavelength of unstable modes indicates that jet stability could be ensured and suitable turbulence be produced. This suggests that shear particle acceleration could represent a viable mechanism for the energization of charged particles in the relativistic jets of AGN. The above considerations are expected to inform our understanding toward a desirable, multiscale treatment (e.g., Marcowith et al. 2020) of particle acceleration in relativistic shearing flows.

We appreciate stimulating discussions with Tony Bell out of which this study grew, and are very grateful to Manel Perucho for comments on an earlier version of the manuscript. We thank the referee for useful comments. F.M.R. acknowledges funding by a DFG Heisenberg Fellowship under RI 1187/6-1.

ORCID iDs

Frank M. Rieger https://orcid.org/0000-0003-1334-2993

References

Berezhko, E. G., & Krymskii, G. F. 1981, SvAL, 7, 352
Birkinshaw, M. 1991, MNRAS, 252, 505
Birkinshaw, M. 1996, Ap&SS, 242, 17
Blandford, R., Meier, D., & Readhead, A. 2019, ARA&A, 57, 467
Blandford, R. D., & Pringle, J. E. 1976, MNRAS, 176, 443
Chhotray, A., Nappo, F., Ghisellini, G., et al. 2017, MNRAS, 466, 3544
De Young, D. S. 1993, ApJ, 402, 95
Earl, J. A., Jokipii, J. R., & Morfill, G. 1988, ApJL, 331, L91
Ferrari, A. 1998, ARA&A, 36, 539
Ferrari, A., Trussoni, E., & Zaninetti, L. 1979, A&A, 79, 190
Giovannini, G., Savolainen, T., Orienti, M., et al. 2018, NatAs, 2, 472
H.E.S.S. Collaboration, Abdalla, H., Adam, R., et al. 2020, Natur, 582, 356
Hamlin, N. D., & Newman, W. I. 2013, PhRvE, 87, 043101
Hanasz, M., & Sol, H. 1996, A&A, 315, 355
Hardee, P. E. 1979, ApJ, 234, 47
Hardee, P. E. 2013, EPJWC, 61, 02001
Hardee, P. E., Rosen, A., Hughes, P. A., & Duncan, G. C. 1998, ApJ, 500, 599
Kimura, S. S., Murase, K., & Zhang, B. T. 2018, PhRvD, 97, 023026
Laing, R. A., & Bridle, A. H. 2014, MNRAS, 437, 3405
Lemoine, M. 2019, PhRvD, 99, 083006
Liang, E., Fu, W., & Böttcher, M. 2017, ApJ, 847, 90
Liu, R.-Y., Rieger, F. M., & Aharonian, F. A. 2017, ApJ, 842, 39
Marcowith, A., Ferrand, G., Grech, M., et al. 2020, LRCA, 6, 1
Martí, J.-M. 2019, Galax, 7, 24
Mertens, F., Lobanov, A. P., Walker, R. C., & Hardee, P. E. 2016, A&A, 595, A54
Perlman, E. S., Biretta, J. A., Zhou, F., Sparks, W. B., & Macchetto, F. D. 1999, AJ, 117, 2185
Perucho, M. 2019, Galax, 7, 70
Perucho, M. 2020, MNRAS, 494, L22
Perucho, M., Hanasz, M., Martí, J.-M., & Miralles, J.-A. 2007, PhRvE, 75, 056312
Perucho, M., Hanasz, M., Martí, J. M., & Sol, H. 2004, A&A, 427, 415
Perucho, M., & Martí, J. M. 2007, MNRAS, 382, 526
Perucho, M., Martí, J. M., & Hanasz, M. 2005, A&A, 443, 863
Rieger, F. M. 2019, Galax, 7, 78
Rieger, F. M., & Duffy, P. 2004, ApJ, 617, 155
Rieger, F. M., & Duffy, P. 2006, ApJ, 652, 1044
Rieger, F. M., & Duffy, P. 2016, ApJ, 833, 34
Rieger, F. M., & Duffy, P. 2019, ApJL, 886, L26
Rossi, P., Mignone, A., Bodo, G., Massaglia, S., & Ferrari, A. 2008, A&A, 488, 795
Sironi, L., Rowan, M. E., & Narayan, R. 2020, arXiv:2009.11877
Tavecchio, F. 2021, MNRAS, in press (doi:10.1093/mnras/staa4009)
Tavecchio, F., & Ghisellini, G. 2015, MNRAS, 451, 1502
Trussoni, E. 2008, in Lecture Notes in Physics, Vol. 754, The Kelvin-Helmholtz Instability, ed. S. Massaglia et al. (Berlin: Springer), 105
Turland, B. D., & Scheuer, P. A. G. 1976, MNRAS, 176, 421
Urpin, V. 2002, A&A, 385, 14
Vega-García, L., Perucho, M., & Lobanov, A. P. 2019, A&A, 627, A79

Webb, G. M. 1989, ApJ, 340, 1112
Webb, G. M., Al-Nussirat, S., Mostafavi, P., et al. 2019, ApJ, 881, 123
Webb, G. M., Barghouty, A. F., Hu, Q., & le Roux, J. A. 2018, ApJ, 855, 31
Webb, G. M., Mostafavi, P., Al-Nussirat, S., et al. 2020, ApJ, 894, 95
Zhang, W., MacFadyen, A., & Wang, P. 2009, ApJL, 692, L40